



Research Article

# Durability performance of alkali-activated concretes exposed to sulfuric acid attack

Anıl Niş<sup>1</sup> \*, Melis Bilenler Altundal<sup>2</sup> 

<sup>1</sup> Department of Civil Engineering, Istanbul Gelisim University, Istanbul (Turkiye), [anis@gelisim.edu.tr](mailto:anis@gelisim.edu.tr),

<sup>2</sup> Department of Civil Engineering, Istanbul Gelisim University, Istanbul (Turkiye), [melisbilenler@hotmail.com](mailto:melisbilenler@hotmail.com)

\*Correspondence: [anis@gelisim.edu.tr](mailto:anis@gelisim.edu.tr)

**Received:** 09.09.2021; **Accepted:** 13.12.2022; **Published:** 30.04.2023

**Citation:** Niş, A., Altundal, M. (2023). Durability Performance of Alkali-Activated Concretes Exposed to Sulfuric Acid Attack. *Revista de la Construcción. Journal of Construction*, 22(1), 16-35. <https://doi.org/10.7764/RDLC.22.1.16>.

**Abstract:** In this research, chemical durability performances of the alkali-activated slag (AAS), 50% ground granulated blast furnace slag and 50% fly ash (AFS), ordinary Portland cement (OPC), and geopolymer (GPC) concretes were investigated thoroughly under 5% sulfuric acid attack. All alkali-activated concrete specimens were produced considering the minimum binder content of 360 kg/m<sup>3</sup> and the maximum alkali activator to binder ratio of 0.45 according to the XA3 environment given in EN 206-1 standard for OPC concrete. The visual inspection, weight change and compressive strength tests were performed to understand the influence of sulfuric acid attack on the resulting performances. Also, scanning electron microscope (SEM) and energy dispersive X-ray spectrometry (EDS) analyses were performed to examine the morphological variations in micro-scale. The mechanical performances and durability of alkali-activated concretes were also compared to the OPC concrete for structural utilization. The results revealed that AFS specimens showed the best durability, while GPC specimens exhibited the poorest durability. SEM/EDS results pointed out that AFS specimens exhibited denser and less porous microstructure, and the reductions in Al/Si and Ca/Si atomic ratios were observed under 5% sulfuric acid attack. In contrast, GPC specimens showed less dense and porous microstructure, and high aluminum leaching was observed. In addition, the wider interconnected macro cracks and high calcium leaching were observed in the AAS samples under 5% sulfuric acid attack. Finally, the AAS and AFS specimens can be utilized in structural applications, while GPC specimens should not be used with a minimum binder content proposed by EN 206-1 standard.

**Keywords:** Geopolymer concrete, alkali activated slag, alkali activated fly ash/slag, alkali-activated concretes, sulfuric acid attack.

## 1. Introduction

The waste material utilization in concrete structures becomes significant for a greener environment in the following years. The production of ordinary Portland cement (OPC) is reported to cause 5-7% of global CO<sub>2</sub> emissions (Benhelal, Zahedi, Shamsaei, & Bahadori, 2013), and OPC production is going to increase with a rise in the world population. The partial use of fly ash, slag, and silica fume is widespread in the concrete industry, and these waste materials are generally used to enhance the durability performance of the OPC (Imbabi, Carrigan, & McKenna, 2013; Tavasoli, Nili, & Serpoosh, 2018). The utilization of waste materials decreases the cement content so that the energy requirement and CO<sub>2</sub> emission decrease. In addition,

the disposal of waste materials from the environment becomes necessary to reduce air pollution. Recently, a novel environmentally friendly concrete called alkali-activated concrete (AAC) has emerged as a cementless type of concrete, and fly ash and ground granulated blast furnace slag have been used as binder materials (Golewski, & Sadowski, 2017). The performance of AAC generally depends on the chemical composition of the used materials (Çevik, Alzebaree, Humur, Niş, & Gülşan, 2018), alkaline activator type and ratio (Ma, Awang, & Omar, 2018; Ryu, Lee, Koh, & Chung, 2013), curing temperature and duration (Niş, & Altındal, 2021; Patil, Chore, & Dodeb, 2014), and binder content (Ibrahim, Johari, Rahman, & Maslehuddin, 2017). In general, fly ash, ground granulated blast furnace slag, and fly ash-ground granulated blast furnace slag incorporated specimens are called as geopolymer (GPC), alkali-activated slag (AAS), and alkali-activated fly ash and slag (AFS), respectively.

For the geopolymerization process, the alkali activators, i.e. sodium silicate and sodium hydroxide, are required for strength enhancement. The GPC specimens require elevated temperatures around 70°C (Soutsos, Boyle, Vinai, Hadjierakleous, & Barnett, 2016; Temuujin, Van Riessen, & Williams, 2009) to have good mechanical strength and durability. In general, GPC specimens show slower strength development compared to AFS and ASS specimens. The activation of fly ash usually depends on the calcium oxide, iron oxide, and reactive silica content (Winnefeld, Leemann, Lucuk, Svoboda, & Neuroth, 2010), particle size distribution, and vitreous phase content (Fernández-Jiménez, Palomo, & Criado, 2005). It was reported in a study that the compressive strength of ambient cured AFS pastes (50%FA+50%S) activated with 10M NaOH solution yielded more than 50 MPa at 28 days, and fly ash/slag ratio was found to be the most significant factor in the strength development (Puertas, Martínez-Ramírez, Alonso, & Vazquez, 2000). The high compressive strength of the AFS specimens depends on the amorphous hydrated alkali-aluminosilicate that comes from fly ash (Palomo, Grutzeck, & Blanco, 1999), and C-S-H gel comes from slag (Chi & Huang, 2013). The formed reaction products of the AFS specimens are the 3D zeolitic gel-type structure due to the activation of fly ash and C-S-H with a dreierketten-type structure due to the activation of slag. For the AAS specimens, the rod-like ettringite and C-S-H type gel are responsible for the strength development and localized at the slag particles (Chi & Huang, 2013).

Researchers focus on the factors affecting the mechanical strength and chemical durability performances of the AAC to use cementless concrete instead of OPC concrete (Aygormez, 2021; Aygormez & Canpolat, 2021). However, due to the lack of knowledge about the mechanical and durability performance of the AAC, the standardization of the AAC for structural utilization has not been completed. Therefore, further studies are required for the utilization of structural concrete elements under chemical environments, especially for the chemical durability performance of AAC.

The sulfuric acid attack can be hazardous to structural reinforced concrete elements of foundations (sulfuric acid including groundwater, resulting from the oxidization of pyrite in backfill) or outer structural column and beam elements, walls, staircases, and slabs at chemical plants or superstructures (acid rain) (Bassuoni & Nehdi, 2007). In a previous study, the chemical durability of the AAC was investigated under seawater, magnesium sulfate, and sulfuric acid environments, and the sulfuric acid attack was found to be the most hazardous environment (Çevik, Alzebaree, Humur, Niş, & Gülşan, 2018). Due to the exposure of structural elements to acidic environments, the durability performance of the AAC under sulfuric acid attack should be investigated. Meanwhile, the XA3 environment is classified as a highly aggressive chemical environment by EN 206-1 standard (EN 206–1 2013), which gives some precautions, i.e., minimum cement content as 360 kg/m<sup>3</sup> and maximum water to cement ratio as 0.45, for the utilization of OPC in XA3 environment. Therefore, for the standardization process of the AAC under highly aggressive chemical environments, the conformity of the XA3 restrictions should also be evaluated.

Considering environmental problems and novel material production economically, this paper focuses on the durability of different environmentally sustainable concretes using minimum binder content and maximum alkaline to binder ratio given in EN 206-1 standard. Therefore, the possible utilization of environmentally sustainable concretes instead of OPC concretes is studied. There is no study in the literature regarding the EN 206-1 standard rules applications to environmentally sustainable concretes. Researchers generally use 500-600 kg/m<sup>3</sup> binder content in sustainable concrete production, which increases alkaline material content. Especially, high alkali content and high molarity of alkaline materials can be hazardous to people (itchy problem, eye contact, i.e.). Therefore, minimum binder and minimum alkaline content use can be significant in the upcoming years for structural applications. For this purpose, the paper is aimed to research the 5% sulfuric acid resistance of the GPC,

AAS, and AFS specimens considering the minimum binder content and maximum alkaline-to-binder ratio according to XA3 condition by EN 206-1 standard for the possible utilization of the AAC instead of OPC. In addition, SEM/EDS analyses were also conducted for the microstructural variations after the acid attack, and the deterioration mechanism of the AAC was correlated to the atomic ratios of the different AAC binder gels.

## 2. Materials and methods

### 2.1. Materials

In the scope of the research, locally available F-type fly ash (FA) conforming to ASTM C618 (ASTM C618-03 2003), and ground granulated blast furnace slag (GGBFS) were utilized as binder materials for the production of fly ash-based geopolymer (GPC), alkali-activated slag (AAS), and alkali-activated fly ash/slag (AFS) specimens. As a reference, OPC concrete was also produced with Type I (CEM I 42.5 R) cement for comparison purposes. A mixture of sodium silicate ( $\text{Na}_2\text{SiO}_3$ ) and sodium hydroxide (NaOH) with a silicate/hydroxide ratio of 2.5 by weight was utilized as an alkaline solution. Commercially available sodium silicate liquid solution with a density of  $1.39 \text{ g/cm}^3$  and alkaline modulus ratio of 2 (Ms:2,  $\text{SiO}_2$ :24%,  $\text{Na}_2\text{O}$ :12%, and the rest is water) was obtained from a local supplier. The sodium hydroxide powder (purity: 97%-98%) was diluted in tap water to produce a 14 M NaOH concentration, which was considered the weakest concentration amount of GPC against chemical exposure (Kumaravel, & Girija, 2013). The natural sand with a specific gravity of  $2.65 \text{ g/cm}^3$  and water absorption of 1.5%, and crushed limestone ( $\leq 4 \text{ mm}$ ) with a specific gravity of  $2.70 \text{ g/cm}^3$  and water absorption of 1.2%, were used as fine aggregates. As coarse aggregates, the No I aggregate with a maximum aggregate grain size of 12 mm, a specific gravity of  $2.71 \text{ g/cm}^3$ , and water absorption of 0.7%, and the No II aggregate with a maximum aggregate grain size of 22 mm, a specific gravity of  $2.72 \text{ g/cm}^3$  and water absorption of 0.6% were utilized. A polycarboxylate ether-based superplasticizer (Yaprho Hyper SCC 900) with a density of  $1,069 \text{ g/cm}^3$  was used to obtain an S4 slump-class concrete. Table 1 summarizes the X-ray fluorescence (XRF) analysis for the chemical composition of the used binder materials.

**Table 1.** The chemical compositions of the materials.

Chemical analysis, %	CaO	$\text{Al}_2\text{O}_3$	$\text{SiO}_2$	$\text{Fe}_2\text{O}_3$	MgO	$\text{SO}_3$	$\text{Na}_2\text{O}$	$\text{K}_2\text{O}$	S.G	L.O.I.
OPC	64.28	4.91	20.17	3.41	1.18	2.84	0.13	0.96	3.14	1.61
Fly ash	1.79	26.37	56.15	6.44	2.35	0.06	1.10	3.80	2.05	2.20
GGBFS	37.92	13.27	37.97	1.16	5.64	0.23	0.84	0.56	2.95	0.01

### 2.2. Mix design and specimen preparation

Material proportions were determined according to EN 206-1 (EN 206-1 2013) and TS13515 (TS13515 2012) (complementary Turkish standard for TS EN 206-1) standards. The minimum cement content and the maximum water-to-cement ratio for OPC specimens are used as  $360 \text{ kg/m}^3$  and 0.45, respectively under the very harsh environmental conditions of XA3. To evaluate the durability performance of GPC, AFS, and AAS specimens under sulfuric acid attack, the minimum fly ash or slag amounts of  $360 \text{ kg/m}^3$  and alkaline solution ( $\text{Na}_2\text{SiO}_3 + \text{NaOH}$ ) to binder ratio of 0.45 were utilized to represent the criteria of XA3 environment by EN 206-1 (EN 206-1 2013) standard. The GPC specimens contain 100% fly ash, the AAS specimens include 100% slag, and the AFS specimens contain 50% fly ash-50% slag labeled as FA100, S100, and FA50S50, respectively. Table 2 represents the mix proportions of the GPC, alkali-activated fly ash/slag concretes, and OPC concrete.

**Table 2.** Mix proportions of the GPC, ASS, AFS and OPC specimens.

Ingredients	Mixture proportions ( $\text{kg/m}^3$ )			
	FA100	FA50S50	S100	OPC
Fly Ash	360	180	0	0
Slag	0	180	360	0
OPC	0	0	0	360
No I (5-12 mm)	560	560	560	560
No II (12-22 mm)	560	560	560	560

Crushed sand	373	373	373	373
Sand	373	373	373	373
Sodium silicate	115.7	115.7	115.7	0
Sodium hydroxide (14M)	46.3	46.3	46.3	0
Superplasticizer	6	6	6	6
Water	25*	31.25*	37.5*	162

\* Water amount in order to obtain similar workability as OPC

The mixing method for the AAC specimens is as follows. First, dry materials (coarse and fine aggregates, binder materials) were added and mixed at 2 min. Then a prepared combination of liquid sodium silicate and 14M sodium hydroxide solution was added into the mixer with a superplasticizer (SP) for additional mixing of 2 min. The prepared 14M NaOH solution was directly used, and the direct use of the alkaline solution is available in the literature (Bondar, Lynsdale, Milestone, Hassani, & Ramezani-pour, 2011; Wongpa, Kiattikomol, Jaturapitakkul, & Chindaprasirt, 2010). In a previous study (Jang, Lee, & Lee, 2014), it was reported that a polycarboxylate ether-based SP improved the workability of the AAC more than the naphthalene-based SP; therefore, a polycarboxylate ether-based SP was utilized in the study. For the AAC specimens, additional water is added to the mixture and mixed for an additional 2 min to obtain similar workability as OPC with an S4 slump class according to EN 206-1 (EN 206-1 2013) standard. For the workability improvement and further geopolymerization, water addition into the AAC can be available in the literature (Albitar, Ali, Visintin, & Drechsler, 2017; Džunuzović, Komljenović, Nikolić, & Ivanović, 2017).

After the mixing procedure, specimens were cast into 150x150x150 mm cubic molds in three layers, and the samples were also compacted on the vibration table for 30 seconds. Next, the specimens were covered with plastic sheets to prevent alkaline loss during curing and kept in the laboratory environment for three days to obtain the required demolding strength due to the low-strength development of the fly ash. Then, the specimens were demolded and cured in an oven at 70°C for 48 h to accelerate the geopolymerization process of FA particles. After oven-curing, AAC specimens were kept in an ambient environment at 28 days. In addition, some of the specimens were also left in an ambient environment without oven-curing to investigate the mechanical strength development of the alkali-activated fly ash/slag concretes in the ambient environment. Therefore, these specimens (without oven-curing) were not evaluated under acid attack. Meanwhile, OPC specimens were cured in a water tank for 28 days for comparison.

### 2.3. Test Method

In this study, the chemical immersion test method was utilized to evaluate the sulfuric acid (H<sub>2</sub>SO<sub>4</sub>) performance of the AAC. After production and curing of the specimens as can be seen in Figs. 1.a and 1.b, specimens were put in containers with enough gaps to satisfy the absorption of solution from all cube surfaces. Meanwhile, the 5% H<sub>2</sub>SO<sub>4</sub> solution was prepared in another container with a volume of 10 lt. Then, the prepared solution was poured slowly into the containers until the 5% H<sub>2</sub>SO<sub>4</sub> solution is above 3 cm from the top of the specimens, and the caps of the containers were closed to prevent the loss of solution evaporation, Fig. 1.c. Also, some of the specimens were left in the ambient environment for comparison. The cube specimens with 150x150x150 mm dimensions were utilized during the chemical tests, and samples were tested at 56. days (28+28) and 90. days (28+62) after the initial 28 days of the curing regime.

There is no standard or accepted test method available to test the sulfuric acid resistance of specimens. Therefore, samples were removed from the acid solutions and waited for 24 h for drying as is seen in Fig. 1.d. The surface photos of the sulfuric acid-exposed specimens were taken for visual inspection. Then, the weights of the specimens were measured to evaluate weight change due to acid exposure, Fig. 1.e. Finally, compressive strength tests were conducted by the ASTM C39 standard (ASTM C39/C39M-01 2003) as shown in Fig. 1.f., and the variations in the compressive strength of the specimens were calculated. The weight change of the samples is also a widely used method in addition to compressive strength test to evaluate the deterioration of the samples under acid attack (Chang, Song, Munn, & Marosszeky, 2005). Furthermore, scanning electron microscope (SEM) and energy dispersive X-ray spectrometry (EDS) analyses were also performed to investigate the morphological variations due to sulfuric acid attack at the microscale level.

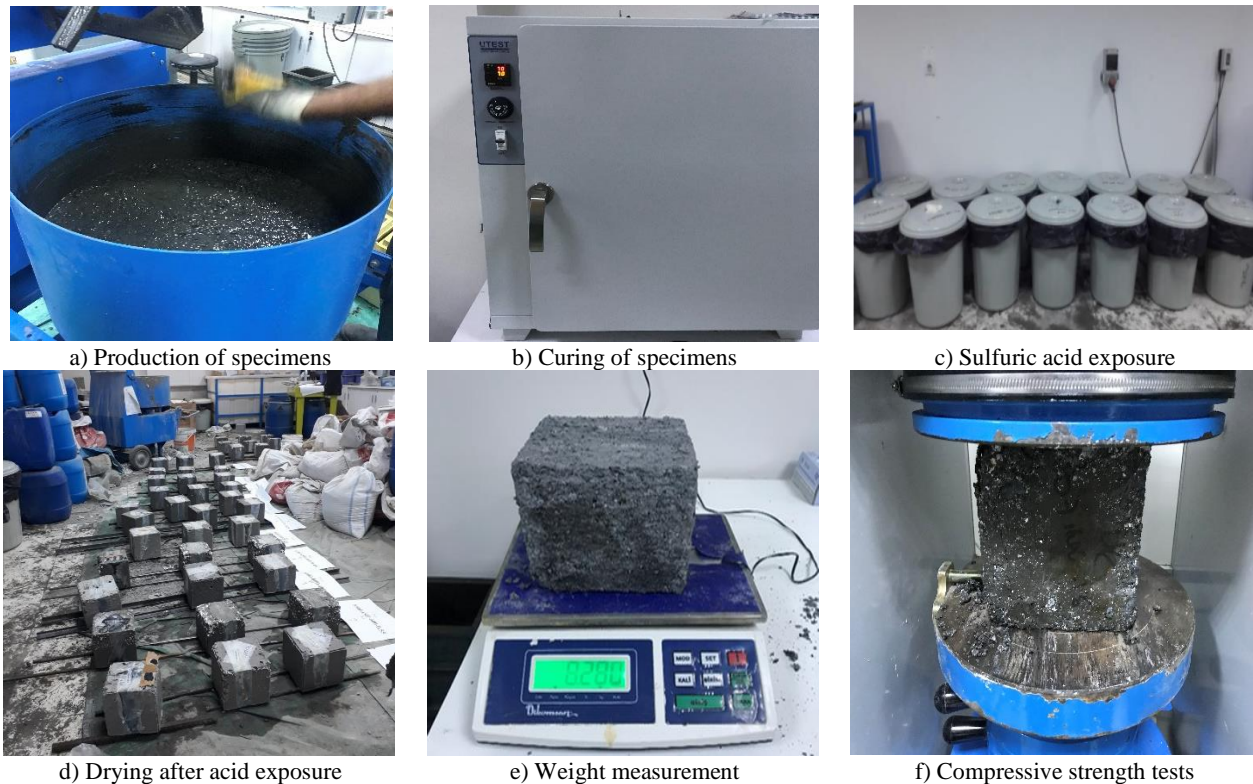


**Figure 1.** Specimen production, curing, and testing after sulfuric acid exposure.

### 3. Experimental results and discussion

#### 3.1. Visual inspection results

Fig. 2 illustrates the visual appearance of specimens under 5% sulfuric acid exposure at 56. and 90. days. The degree of deterioration increased with an increase in acid exposure time. The softening was observed on the specimen surfaces due to the sulfuric acid attack. The OPC concrete showed significant loss of cement mortar from the surface, indicating the most severe damage. The GPC specimens also showed serious deterioration by forming severe white deposits on the specimen surface, and the expansion of the GPC mortar from coarse aggregates was observed. The AAS specimens showed moderate surface erosion, and spalling occurred at the corner of the cube specimens. The AFS specimens showed the least deterioration by forming fewer white deposits on the specimen surface, and a negligible amount of surface erosion was observed on the specimen surface. The AFS specimens showed the best visual durability performance against the 5% sulfuric acid solution. The highest deterioration on the surfaces of OPC specimens can be attributed to the high CaO amount in the cement phase. The severe deterioration of GPC specimens due to the low CaO content may be resulted from the increased porosity due to the unreacted fly ash particles in the GPC matrix.

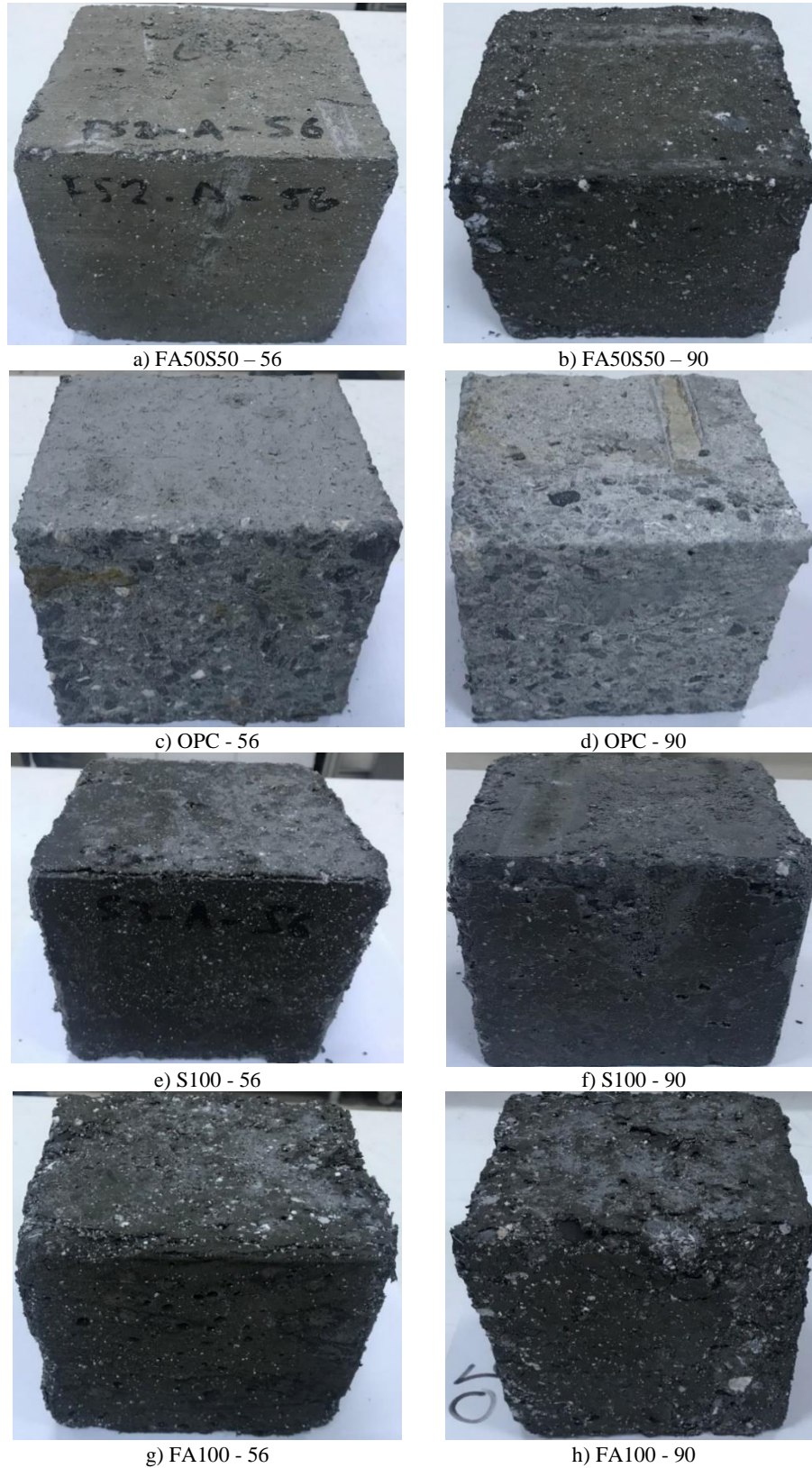


**Figure 2.** Visual appearance of the specimens after 5% sulfuric acid exposure at 56 and 90 days.

### 3.2. Weight change results

Table 3 illustrates the average weights, weight loss index (WLI-%), and weight gain index (WGI-%) of the specimens under ambient and sulfuric acid environments. The weight loss index (WLI) is a relative (%) weight change of the specimens after a specified acid exposure time with respect to the initial specimen weight. The weight gain index (WGI) is a relative (%) weight change of the specimens after a specified acid exposure time with respect to the weights of the unexposed specimens in the same period. Similar parameters for the compressive strength evaluation were used in the previous study (Džunuzović, Komljenović, Nikolić, & Ivanović, 2017).

In the scope of the study, weight change index parameters were proposed and used. The results showed that weight loss was observed for FA100, OPC, and S100 specimens under the ambient environment for two months due to the ongoing reactions. The weight reduction of alkali-activated concretes in an ambient environment due to the ongoing geopolymerization reactions was also reported in earlier investigations (Li & Ding, 2003; Li & Roy, 1988). A slight weight gain was observed for the AFS specimens, indicating the completion of the geopolymerization reactions due to oven curing. In addition, the highest weight reduction was observed for the GPC specimens, indicating an ongoing geopolymerization process even though the oven curing method (70°C for 48h). The ongoing geopolymerization reactions in GPC specimens after oven curing was also reported in the literature (Bakharev, 2005; Palomo, Grutzeck, & Blanco, 1999).

**Table 3.** Weights, WLI (%) and WGI (%) of the specimens under ambient and acid environments.

Days	Weight loss index <sup>1</sup> (WLI-%)				Weight gain index <sup>2</sup> (WGI-%)			
	S100	FA50S50	OPC	FA100	S100	FA50S50	OPC	FA100
28	100.00	100.00	100.00	100.00	100.00	100.00	100.00	100.00
56 (28+28)	99.29	99.83	100.29	99.31	99.04	99.99	100.37	99.72
90 (28+62)	99.6	100.36	99.36	99.12	99.88	99.95	99.63	101.84

<sup>1</sup>Weight loss index (WLI) (%) – Percentage of weight of the specimens under sulfuric acid ( $W_{(28+t)}$ ) after a specified acid exposure time (28+t; t=28, 62 days) with respect to initial weight of the specimens after 28 days ( $W_{(28)}$ ) –  $(W_{acid(28+t)} / W_{(28)}) * 100$  (%)

<sup>2</sup>Weight Gain Index (WGI) (%) – Percentage of weight of the specimens after a specified acid exposure time ( $W_{(28+t)}$ ) with respect to the unexposed (reference) specimens in the same period of time –  $(W_{acid(28+t)} / W_{ambient(28+t)}) * 100$  (%)

The specimens exposed to the sulfuric acid solution after 90 (28+62) days showed that WLI-% becomes 99.6 for S100, 100.36 for FA50S50, 99.36 for OPC, and 99.12 for FA100 specimens. WLI-% results showed that the weight loss becomes in the range of GPC > OPC > AAS > AFS specimens. The weight gain was observed for the FA50S50 specimens since extra pores occurred in the specimens resulting from the oven-curing at 70°C for 48h. After sulfuric acid exposure, these pores absorbed the chemical solution, increasing the weight of the specimens. Similar results were also obtained in earlier research (Attigbe & Rizkalla, 1988; Mehta & Siddique, 2017; Thokchom, 2014). In addition to WLI-%, WGI-% can also be used to determine the weight change of the specimens since the weight of the specimens also changes with time for the control (unexposed) specimens due to the ongoing geopolymerization reactions. Similar to WLI-%, WGI-% results also indicated that weight loss becomes in the ranges of GPC > OPC > AAS > AFS specimens. However, the weight change results became smaller or different for this case since the reduction in weight results resulted from the acid exposure and the ongoing hydration reactions.

For the FA100 specimens, WGI-% was observed to be higher than 100% since weight reduction under the ambient environment becomes higher than the weight reduction under sulfuric acid solution, which can be attributed to the chemical solution absorption of the pores of the GPC specimens. The results showed that WGI-% should be used when determining the weight change of the specimens since continuous hydration reactions may yield misleading results, especially for the fly ash-based GPC specimens.

### 3.3. Compressive strength test results

Figs. 3 and 4 present the average compressive strengths of the specimens at 28, 56, and 90 days. In addition, some of the specimens were also left in the ambient environment without heat curing to observe the compressive strength development for the GPC, AFS, and AAS specimens for 28 days under the ambient environment, and the results were given as 28 NH (no-heat applied). The compressive strengths of the S100, FA50S50, OPC, and FA100 specimens without heat curing (28NH) were 74.77 MPa, 54.58 MPa, 49.58 MPa, and 16.1 MPa at 28 days. Meanwhile, the compressive strengths of the oven-cured S100, FA50S50, OPC, and FA100 specimens at 28 days were 78.34 MPa, 71.61 MPa, 49.58 MPa, and 22.36 MPa at 28 days. The differences between with/without heat curing for the AAS, AFS and GPC specimens were 5%, 24%, and 28%, respectively at 28 days. Results indicated that AAS specimens can be used in-situ applications without heat curing even lower slag (360 kg/m<sup>3</sup>) amounts.

However, low compressive strength values were obtained for GPC specimens with/without heat curing when low fly ash content (360 kg/m<sup>3</sup>) was used. For the AFS specimens, the inclusion of slag on fly ash-based specimens had a favorable effect of eliminating heat curing. The compressive strength increase becomes significant even under low slag dosages. OPC specimens exhibited lower compressive strength values than the AAS (with/without heat curing) and AFS (with heat curing) specimens. Also, similar compressive strengths were obtained in between AFS specimens without heat curing and OPC specimens. Meanwhile, OPC specimens showed higher compressive strengths than the GPC specimens (with/without heat curing).

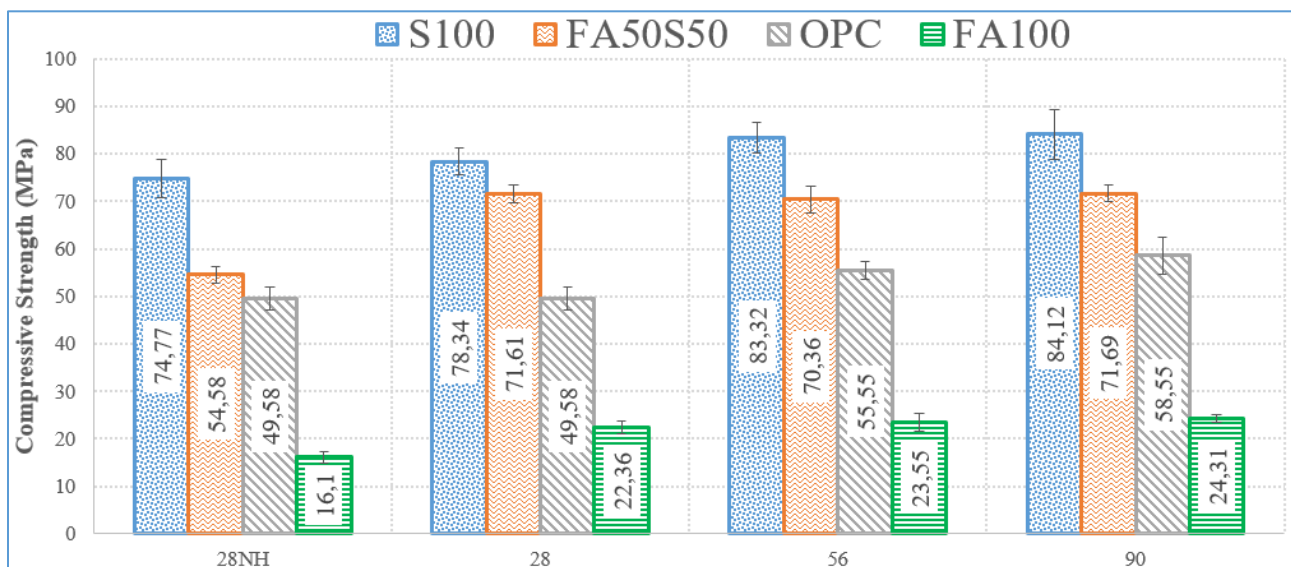


Figure 3. Compressive strengths of the specimens at ambient environment.

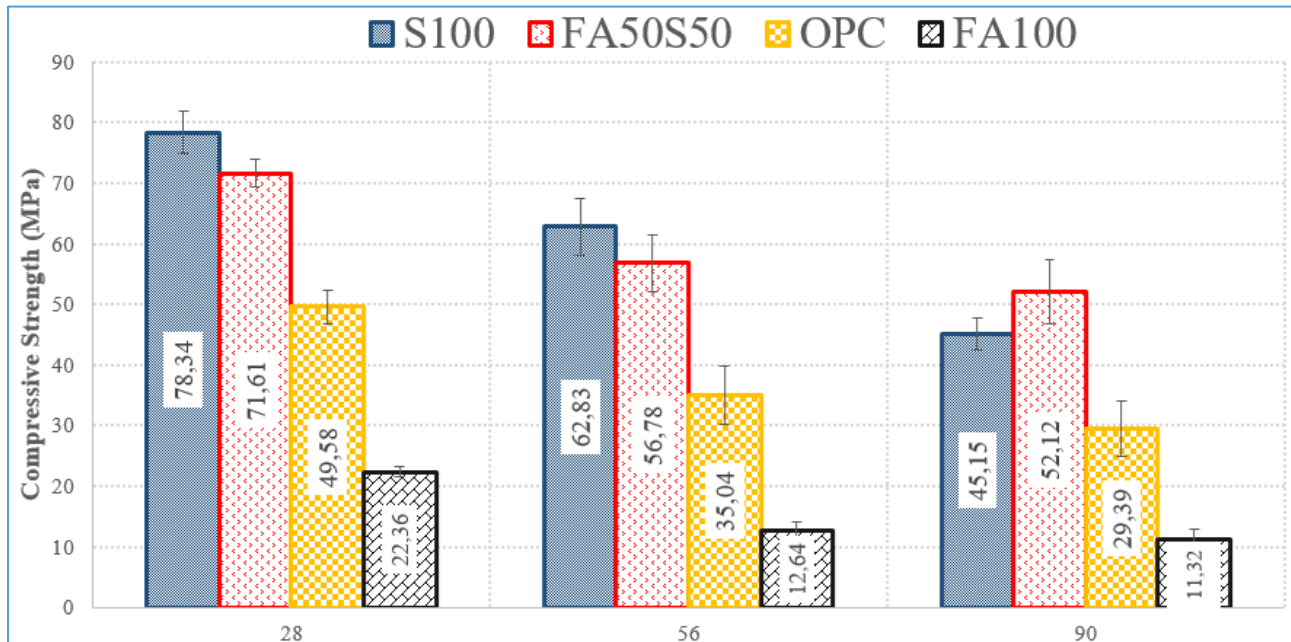


Figure 4. Compressive strengths of the specimens at 5% sulfuric acid environment.

The compressive strengths of the S100, FA50S50, OPC, and FA100 specimens were 83.32 MPa, 70.36 MPa, 55.55 MPa, and 23.55 MPa at 56 days, and they were 84.12 MPa, 71.69 MPa, 58.55 MPa, and 24.31 MPa at 90. days, respectively. The results showed that compressive strengths of the alkali-activated concrete specimens continued to increase with age even after the heat-curing application, except for the FA50S50 specimens. The results indicated that the compressive strengths of the GPC and AAS specimens under the ambient environment increased with time despite the initial heat curing at 70°C for 48h. It was stated in another investigation (Wardhono, Gunasekara, Law, & Setunge, 2017) that the compressive strength increase was stabilized 56 days later for the AAS specimens even without oven-curing, while compressive strength increase continued up to 540 days despite initial oven curing of 80°C at 24 h for the GPC specimens. Similar results were also obtained in this research due to the ongoing geopolymerization process for the GPC specimens.

The compressive strength increase was 5% and 9% at 56. and 90. days for GPC specimens. In contrast, the compressive strength increase was stabilized for the AAS specimens 56 days later since strength enhancement was 6% and 7% at 56. and 90. days, respectively. For the AFS specimens, compressive strength improvement was almost stabilized for 28 days since no strength improvement was observed for the later ages. The compressive strength of the acid-exposed specimens decreased with increasing exposure time. The compressive strengths of the S100 specimens reduced from 78.34 MPa at 28 days to 62.83 MPa at 56 days (28 days of acid exposure) and 45.15 MPa at 90. days (62 days of acid exposure). Similarly, the compressive strengths of the FA50S50 specimens reduced from 71.61 MPa at 28 days to 56.78 MPa at 56 days and 52.12 MPa at 90. days. For the OPC specimens, compressive strengths at the ambient environment became 49.58 MPa, while they reduced to 35.04 MPa at 56 days and 29.39 MPa at 90 days at 5% sulfuric acid attack. Finally, the lowest compressive strength of FA100 specimens (22.36 MPa) decreased to 12.64 MPa and 11.32 MPa at 56 and 90 days.

Table 4 illustrates the strength loss index (SLI-%) and strength gain index (SGI-%) of the specimens under ambient and sulfuric acid environments. The strength loss index (SLI-%) is a relative (%) compressive strength variation of the specimens after a specified acid exposure time with respect to initial compressive strength. The strength gain index (SGI-%) is a relative (%) compressive strength variation of the specimens after a specified acid exposure time with respect to the compressive strengths of the unexposed (reference) specimens in the same period. The strength loss index (SLI-%) due to sulfuric acid attack was found to be 80.20 and 57.63 for S100, 79.29 and 72.78 for FA50S50, 70.67 and 59.28 for OPC, and 56.53 and 50.63 for FA100 specimens for 28+28 and 28+62 days, respectively. The SLI-% results increased as GPC (51) > AAS (58) > OPC (59) > AFS (73) at the end of the acid exposure period. Meanwhile, the strength gain index (SGI-%) due to the acid

exposure was 75.41 and 53.67 for AAS, 80.70 and 72.70 for AFS, 63.08 and 50.20 for OPC, and 53.67 and 46.57 for GPC specimens for 28+28 and 28+62 days, respectively. The SGI-% results increased as GPC (47) > OPC (50) > AAS (54) > AFS (73). The SLI-% and SGI-% results were found similar for the AFS specimens since geopolymerization reactions were almost completed at 28 days. However, SGI-% results become different than SLI-% results when ongoing hydration reactions take place. Therefore, SGI-% results were found more accurate, which should be used to evaluate the durability performance of the specimens instead of SLI-% results. Durability results indicated that the least sulfuric acid resistance was obtained on the GPC specimens, while AFS specimens showed superior performance under sulfuric acid attack. The compressive strength reduction due to acid exposure can be attributed to the ratio of the deteriorated cross-section to the sound cross-section since the acid-deteriorated surface showed weak mechanical properties (Bassuoni, & Nehdi, 2007). The visual inspection results also confirmed the compressive strength test results that the most sulfuric acid-influenced concrete of GPC showed the lowest compressive strength. In contrast, the least visually deteriorated AFS concrete exhibited superior mechanical strength. The least sulfuric acid resistance of GPC can be attributed to the unreacted fly ash particles, cracks in the microstructure, and weak interfacial zone due to voids as is seen in Figs. 5 and 6.

**Table 4.** Compressive strengths (CS), SLI-% and SGI-% of the specimens under ambient and acid environments.

Days	Strength Loss Index (SLI-%)				Strength Gain Index (SGI-%)			
	S100	FA50S50	OPC	FA100	S100	FA50S50	OPC	FA100
28	100.00	100.00	100.00	100.00	100.00	100.00	100.00	100.00
56 (28+28)	80.20	79.29	70.67	56.53	75.41	80.70	63.08	53.67
90 (28+62)	57.63	72.78	59.28	50.63	53.67	72.70	50.20	46.57

<sup>1</sup>Strength loss index (SLI-%) – Percentage of compressive strength of the specimens under sulfuric acid ( $\sigma_{(28+t)}$ ) after a specified acid exposure time (28+t; t=28, 62 days) with respect to initial strength of the specimens after 28 days ( $\sigma_{(28)}$ ) –  $(\sigma_{acid(28+t)} / \sigma_{(28)}) * 100$  (%)

<sup>2</sup>Strength gain index (SGI-%) – Percentage of compressive strength of the specimens after a specified acid exposure time ( $\sigma_{(28+t)}$ ) with respect to the unexposed (reference) specimens in the same period of time –  $(\sigma_{acid(28+t)} / \sigma_{ambient(28+t)}) * 100$  (%)

The low compressive strength and higher deterioration of the heat-cured GPC specimens under sulfuric acid exposure can be attributed to; i) low fly ash content, ii) alkali activator type and amount, and iii) low CaO content in fly ash particles. In a study (Ridtirud, Chindaprasirt, & Pimraksa, 2011), the optimum SS/SH ratio on compressive strength of the mortar geopolymer specimen was evaluated, and the compressive strengths were found to be 25 MPa, 28 MPa, 42 MPa, 45 MPa, and 23 MPa for the SS/SH ratio of 1/3, 2/3, 1, 3/2, and 3/1, respectively. A considerable compressive strength reduction was observed for the fly ash-based geopolymer specimens with an SS/SH ratio of 3, and the optimum ratio for the SS/SH was found to be 1.5. In another study, 100% SS, 75% SS + 25% SH, 50% SS + 50% SH, 25% SS + 75% SH, and 100% SH were utilized, and the compressive strengths were found to be 13 MPa, 32 MPa, 43 MPa, 23 MPa, and 14 MPa, respectively (Ryu, Lee, Koh, & Chung, 2013). Results showed that alkaline activator content is a significant parameter, and the reduction of compressive strength can be expected when SS/SH ratio becomes higher than 2. The improved compressive strength for the SS/SH ratio of smaller than 2 may result from the increasing Na content since Na ions take place at the geopolymerization process as a charge-balancing ion. For the higher SS/SH ratios (>2), both the water escape and formation of 3D aluminosilicate geopolymer networks are hindered, which inhibits the geopolymerization, resulting in a decrease in the mechanical strength due to increased insoluble sodium silicate content (Gao et al., 2014; Part, Ramli, & Cheah, 2015; Reddy, Dinakar, & Rao, 2018).

The fly ash content (binder amount) is also a significant parameter, influencing the mechanical strength and durability of specimens. In a study (Wardhono, Gunasekara, Law, & Setunge, 2017), a similar alkaline modulus of 2 and a slightly higher fly ash content of 409 kg/m<sup>3</sup> with 15 M NaOH concentration was utilized, and the compressive strengths were found to be 22.4 MPa, 25.1 MPa, 27 MPa, and 33.2 MPa at 28, 56, 90 and 540 days, respectively, slightly higher compressive strength values than this study. In addition, in the previous work (Çevik, Alzebaree, Humur, Niş, & Gülşan, 2018), a similar alkaline modulus of 2, a SS/SH ratio of 2.5, a liquid to binder ratio of 0.45, and 14 M NaOH was utilized. The GPC specimens were produced with a binder amount of 500 kg/m<sup>3</sup> (higher than 360 kg/m<sup>3</sup>), and the average compressive strength was found 45 MPa for 28 days. In the same research, the compressive strength decreased to 32 MPa (28% reduction) after one month of exposure to sulfuric acid, and this reduction (28% reduction) was found low than the OPC specimens (34% reduction) with a

water/cement ratio of 0.45. Furthermore, the effect of low calcium content was also examined (Çevik, Alzebaree, Humur, Niş, & Gülşan, 2018; Kurtoglu et al., 2018) and found that GPC specimens having low CaO showed lower compressive strength and less mechanical deterioration. In this study, fly ash content is reduced to  $360 \text{ kg/m}^3$  (below the limit value of XA3 condition for EN 206-1). The findings revealed that the compressive strength of the GPC specimens diminished with decreasing fly ash content as expected, while deterioration amount increased even though low CaO including GPC specimens. This can be attributed to a less dense microstructure due to the unreacted fly ash particles, further explained in the microstructural evaluation part.

The least deterioration was observed on FA50S50 specimens, indicating that sufficient CaO content comes from the slag particles so that a denser structure (C-S-H) was obtained and a reduction in the compressive strength loss was obtained under acid attack. The calcium ions inside the slag particles may enter into the fly ash-based geopolymer matrix (Si-O-Al-O) to form C-(A)-S-H gel structure and contribute to the development of compressive strength of the AFS system. In addition to the C-S-H type gel structure formation, the finer unreacted slag particles (finer than fly ash) reduce porosity by filling the pores (Al-Majidi, Lampropoulos, Cundy, & Meikle, 2016) and decrease the acid penetration into the core of the specimens. As a result, a higher unaffected core region yields higher mechanical strength of the AFS structures.

For the AAS system, higher deterioration was observed due to the higher Ca-rich gel structure. However, the reduction amount in the compressive strength (or SGI-%) due to the acid attack was found less than OPC specimens, indicating AAS specimens showed better chemical durability resistance than OPC specimens when low slag content ( $360 \text{ kg/m}^3$ ) was utilized. It was also reported in the previous study (Kurtoglu et al., 2018) that AAS specimens with higher slag content ( $500 \text{ kg/m}^3$ ) also showed better mechanical and durability performance than the OPC specimens. The highly cross-linked C-A-S-H gel with a higher bound water content exists in the AAS structures, while the low bound water content of N-A-S-H gel formed in the GPC structures (Juenger, Winnefeld, Provis, & Ideker, 2011). Due to the more bound water (AAS) and more CaO content, more filling capacity was observed in AAS specimens, which decreased porosity and improved durability. Also, low-bound water in the GPC specimens increased porosity and poor durability (Provis, Myers, White, Rose, & Deventer, 2012).

#### 3.4. Scanning electron microscopy (SEM) results

Figs. 5 and 6 show the SEM images of the AAS, AFS, OPC, and GPC specimens under ambient and sulfuric acid environments, respectively, at 90 days. AAS micrographs illustrated well-distributed paste with less embedded unreacted slag grains (irregular-shaped), indicating denser and homogeneous microstructure. Most of the slag grains have been dissolved by the alkali activators, forming a C-S-H gel with the silica from the alkali activators at 90 days, as shown in Fig. 5.a. However, wider interconnected macro cracks were observed in the AAS microstructure as shown in Fig. 5.a due to the water evaporation and self-desiccation during oven curing (Wardhono, Gunasekara, Law, & Setunge, 2017) and shrinkage of the reaction products (Lee, Jang, & Lee, 2014). AFS micrographs at 90 days showed a denser and homogenous binding phase with a low amount of unreacted fly ash and slag particles, as is seen in Fig. 5.b. The microstructure of fly ash consists of spherical vitreous particles of different sizes, while the microstructure of slag consists of irregular-shaped and sharp-edged with rough surface, Fig. 5.b. The continuous binding paste of AFS specimens seems similar to AAS micrographs, which indicates that C-S-H type gel is predominant in the AFS microstructure (Ismail et al., 2014). Fewer amount of cavities and narrower micro cracks were observed in the microstructure of the AFS specimens (Fig. 5.b), decreasing porosity and harmful ion permeability.

The 90-day cured fly ash-based GPC micrographs show large quantities of unreacted spherical fly ash particles with different particle sizes with smooth texture, indicating the incomplete geopolymerization process. The heterogeneously distributed cavities also exist in the binding paste, resulting in a more porous microstructure, as illustrated in Fig. 5.d. In addition, the GPC microstructure includes great numbers of voids and microcracks, which would spread further and form a porous microstructure (Mehta & Siddique, 2017). In an earlier investigation, it was reported that unreacted fly ash particles do not fill the voids. Instead, they improve the strength with time via improving bonding strength due to the complex reaction among the surfaces of the fly ash particles (Kumar, Kumar, & Mehrotra, 2007). Meanwhile, the OPC microstructure is illustrated in Fig. 5.c. The OPC micrographs indicated no signs of unreacted particles, cracks, voids, and well-distributed paste with hydration gel products, resulting in a denser and homogeneous microstructure.

The microstructures of the specimens indicated that GPC specimens look porous due to poor adhesion of the unreacted spherical fly ash particles (Fig. 5.d). Meanwhile, the microstructure of AAS specimens appears to be homogeneous and denser, but they have wider interconnected self-desiccation cracks (Fig. 5.a). Therefore, both microstructures seem inherently weak. Meanwhile, for the AFS specimens, the binder phase appears to be denser and homogenous and lacks the self-desiccation cracks as in the case of the AAS specimens. It can be attributed to the addition of aluminum comes from FA particles, which caused stronger and non-granular gel that does not shrink as in the case of AAS (Soutsos, Boyle, Vinai, Hadjierakleous, & Barnett, 2016). For this reason, the AFS microstructure seems to be the best microstructure and showed the best performance against sulfuric acid attacks.

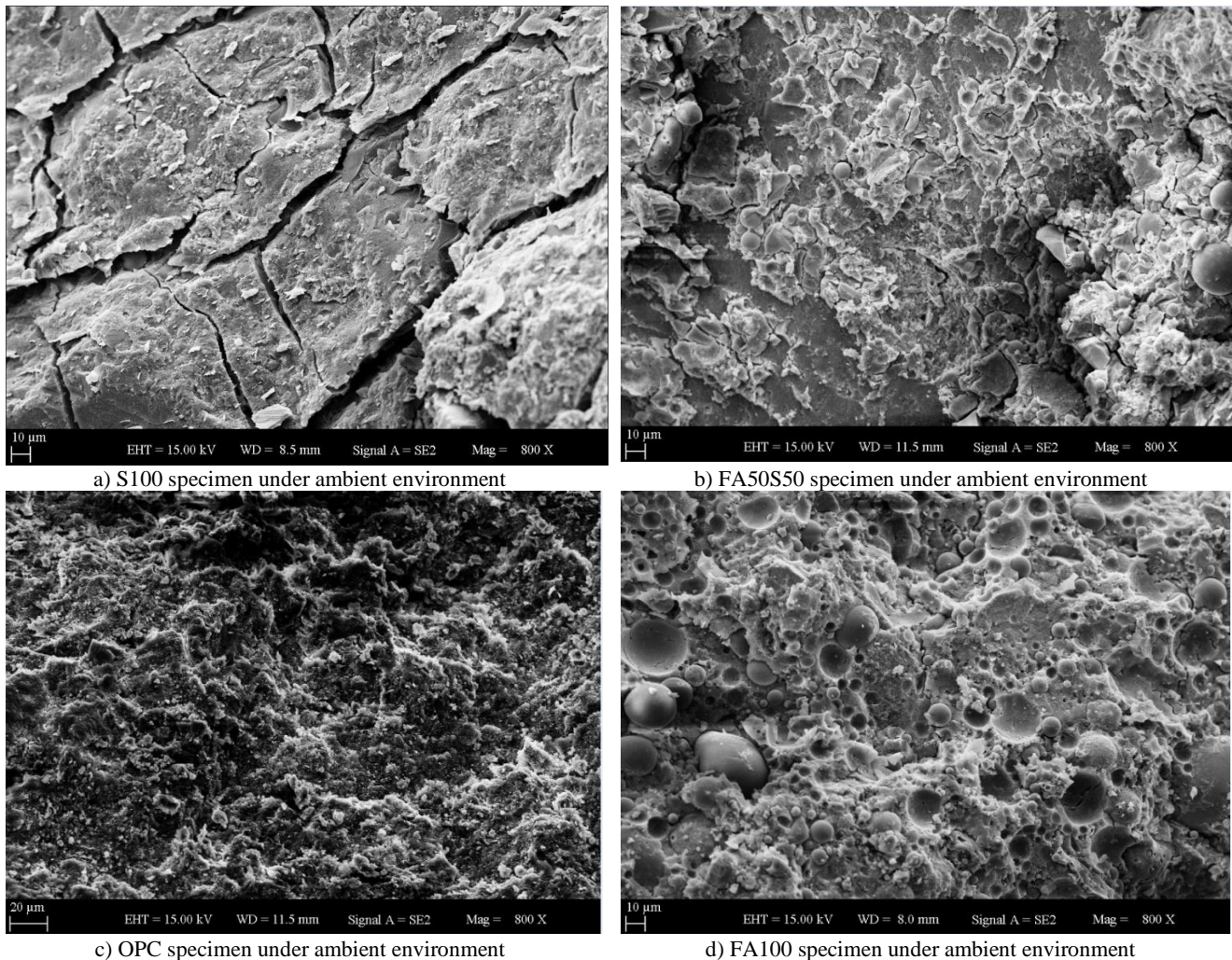
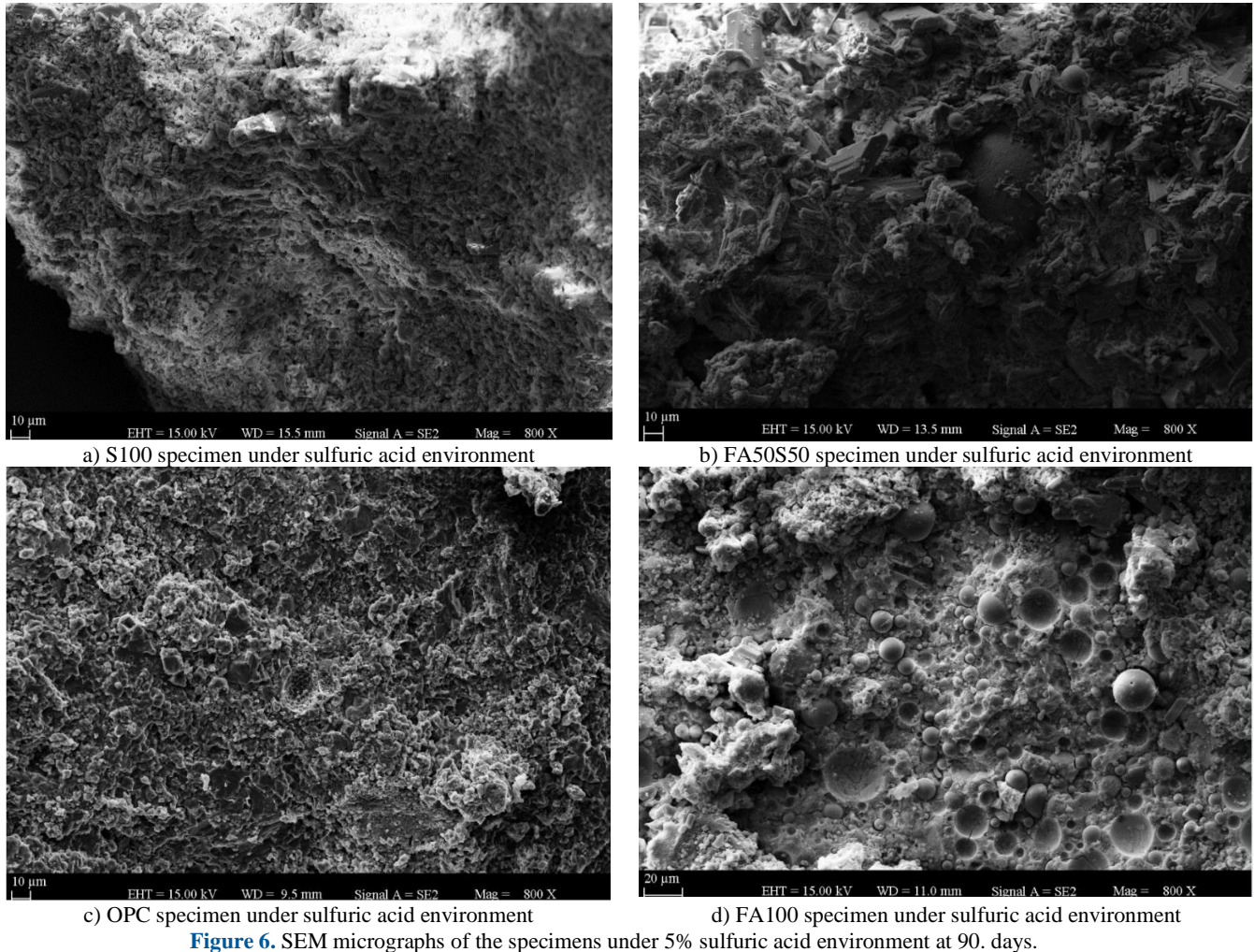


**Figure 5.** SEM micrographs of the specimens under ambient environment at 90. days.



For the sulfuric acid-exposed specimens, the microstructure of the acid-exposed GPC specimens was found similar to the unexposed specimens, Fig. 6.d. A similar observation was also reported in the earlier study (Zhang, Yao, Yang, & Zhang, 2018). In general, the main deterioration mechanism is the reaction products between calcium and sulfuric acid, resulting in lower compressive strength values as in the AAS and AFS specimens. However, due to the low calcium content in the GPC specimens, the formation of reaction products was lower than AFS and AAS specimens.

For the GPC specimens, the main deterioration mechanism can be attributed to the deterioration of strong Al-O and Si-O bonds due to the penetration of harmful sulfate ions inside the geopolymeric binders and/or the loss of adhesion and disintegration between geopolymeric binders and aggregates (Mehta & Siddique, 2017). With slag incorporation, AFS and AAS microstructures become denser, and no or limited cracks were observed in the corroded layers. It may be attributed to the existence of calcium-based reaction products, which cause the formation of harmful calcium sulfates, as shown in Figs. 6.a - 6.c. The EDS results also confirm that sulfur products emerge at the corroded microstructures, which can fill the micro cracks. The occurrence of gypsum was expected in SEM micrographs after sulfuric acid exposure; however, it was not clearly observed. A similar observation was also reported in another study that gypsum was not observed in SEM micrographs but it was found in the XRD results (Zhang, Yao, Yang, & Zhang, 2018). In the same study, limited microcracks in the corroded microstructure are attributed to the reduced capillary stress, resulting from the immersion condition of specimens in the sulfuric acid (Zhang, Yao, Yang, & Zhang, 2018).

### 3.5. Energy-dispersive X-ray Spectroscopy (EDS) Results

Table 5 summarizes the EDS results of the alkali-activated concretes for the gel binder regions (unreacted fly ash and slag particle results excluded) for the different studies in the literature. In this study, the average atom ratios of the gel binder for the GPC specimens, AFS specimens, and AAS specimens were also given in Table 5. For the uncorroded GPC specimens, N-A-S-H type gel was formed with a low Ca/Si ratio. The Al/Si, Na/Si, and Na/Al ratios were 0.46, 0.16, and 0.35, respectively, for the geopolymer binder gel. After sulfuric acid exposure, Al/Si atomic ratio significantly decreased from 0.46 to 0.30, while Na/Al atomic ratio slightly reduced from 0.35 to 0.29 and Na/Si atomic ratio slightly increased from 0.16 to 0.20 for corroded GPC specimens. The sulfur amounts increased from 0.99% to 13.96% after exposure to the sulfuric acid attack.

For the uncorroded alkali-activated fly ash/slag-based (AFS) specimens, C-N-A-S-H type gel was formed with a Ca/Si ratio of 0.7. The increase in the calcium content after the incorporation of slag was also reported in the literature (Marjanović, Komljenović, Baščarević, Nikolić, & Petrović, 2015; Zhang, Yao, Yang, & Zhang, 2018). The Al/Si, Na/Si, and Na/Al ratios were 0.36, 0.42, and 1.15, respectively, for the AFS binder gel. After sulfuric acid exposure, Al/Si, Na/Al and Na/Si atomic ratios of corroded specimens slightly decreased from 0.36 to 0.29, 1.15 to 0.9, and 0.42 to 0.39, respectively. Due to the sulfuric acid attack, the sulfur compounds increased from 1.48% for uncorroded specimens to 15.39% for corroded specimens.

In the reference samples of the alkali-activated slag (AAS) specimens, C-A-S-H type gel formed with a Ca/Si ratio of 1.05. The highest calcium content was found in AAS specimens due to the high slag content. The Al/Si, Na/Si, and Na/Al ratios were 0.30, 1.57, and 2.35, respectively, for the AAS binder gel. For the acid-corroded AAS specimens, Al/Si, Ca/Si, and Na/Si atomic ratios slightly decreased from 0.30 to 0.26, 1.05 to 0.92, and 1.57 to 1.42, while Na/Al atomic ratio significantly increased from 2.35 to 4.75. A similar increase in the Na/Al atomic ratio after the sulfuric acid attack was also reported in the earlier study (Zhang, Yao, Yang, & Zhang, 2018). This was attributed to the leaching of the alkali ions from the interior binder, and the accumulation of the pore solution resulted from the blocking effect of the formed gypsum. In general, the C-A-S-H decalcifies when the sulfate attack continues, decreasing the Ca/Si ratio. In this study, decalcification also occurred only in the AAS binder after two months of exposure to the 5% sulfuric acid attack. Decalcification was also reported in the previous study (Allahverdi & Skvara, 2005).

The sulfur compound was also found to be highest in AAS specimens, which was increased from 1.61% for uncorroded specimens to 17.19% for corroded specimens. In an earlier investigation, sulfur compounds were found to be maximum at higher calcium incorporating specimens (%30 OPC in addition to fly ash-based GPC) after the sulfuric acid attack (Mehta & Siddique, 2017). A similar finding was also found in this study that the highest sulfur content can be attributed to the reaction between sulfuric acid and high calcium in AAS specimens. The reduction in Na/Al ratio lowers the geopolymerization reactions so that thermal cracks decrease for the slow geopolymer reactions. In GPC specimens, fewer micro cracks are observed than the AAS specimens due to the lower Na/Al atomic ratio of fly ash particles.

**Table 5.** EDS results of the alkali-activated concretes for the gel binder regions.

Slag content (%)	Layer	Na/Al	Al/Si	Ca/Si	Na/Si	Sulfur (%)
0 (FA100)	Corroded	0.29	0.30	0.06	0.20	13.96
	Uncorroded	0.35	0.46	0.04	0.16	0.99
50 (FA50S50)	Corroded	0.90	0.29	0.74	0.39	15.39
	Uncorroded	1.15	0.36	0.71	0.42	1.48
100 (S100)	Corroded	4.75	0.26	0.92	1.42	17.19
	Uncorroded	2.35	0.30	1.05	1.57	1.61

SEM/EDS analysis results also showed that the atomic ratios of the Na/Al, Al/Si, Ca/Si, and Na/Si were similar to the literature findings given in Table 6. It is indicated that the highest Ca/Si ratio was observed in AAS specimens, while the highest Al/Si ratio was observed in GPC specimens. The Na/Si atomic ratio was found to be higher for the AAS specimens than the AFS and GPC specimens, respectively. The SEM/EDS results pointed out that the Al/Si atomic ratio was found to

be decreased after the sulfuric acid attack for AAS, AFS, and GPC binder gel, which can be attributed to aluminum leaching from gel structure as a result of proton attack on the Si-O-Al network (Allahverdi & Skvara, 2001). However, the highest decrease in Al/Si atomic ratio was observed in GPC specimens, which can be an indicator of the highest deterioration of the Si-O-Al network due to the sulfuric acid attack. After slag incorporation, the decrease in Al/Si atomic ratio was found smaller for AFS and AAS specimens, which indicates that a dense matrix prevents the aluminum loss from gel structure after the acid attack (Zhang, Yao, Yang, & Zhang, 2018). For the ASS specimens, the high degradation under acid attack can be attributed to the loss of aluminum and decalcification (the highest decrease in the Ca/Si ratio). The least deterioration of the AFS specimens can be attributed to the least decrease in Al/Si and Ca/Si atomic ratios.

**Table 6.** EDS results of different alkali-activated materials in the literature.

a) Alkali activated fly ash and slag materials under 3% sulfuric acid solutions (Zhang, Yao, Yang, & Zhang, 2018).					
Slag content (%)	Layer	Na/Al	Al/Si	Ca/Si	
0	Corroded	0.26	0.24	0.02	After 28 days of ambient curing, specimens were left to 28 days under 3% sulfuric acid attack. Alkali Solution: Na <sub>2</sub> SiO <sub>3</sub> + 10 M NaOH
	Uncorroded	0.28	0.68	0.03	
30	Corroded	0.61	0.2	0.3	
	Uncorroded	0.79	0.36	0.37	
70	Corroded	0.6	0.25	0.85	
	Uncorroded	1.82	0.31	0.85	
100	Corroded	6.18	0.25	0.93	
	Uncorroded	3.2	0.26	1.02	

b) Alkali activated fly ash and slag based materials under ambient environment (Lee, Jang, & Lee, 2014).					
Slag content (%)	Layer	Na/Si	Al/Si	Ca/Si	Curing: 60°C at 24 h. Specimens were tested after 28 days. Alkaline solution: Sodium Silicate powder
10	Uncorroded	0.37	0.33	0.26	
20	Uncorroded	0.29	0.35	0.46	
30	Uncorroded	0.26	0.36	0.53	

c) Alkali activated fly ash and slag based materials under ambient environment (Soutsos, Boyle, Vinai, Hadjierakleous, & Barnett, 2016).					
Slag content (%)	Layer	Na/Si	Al/Si	Ca/Si	Curing: 70°C at 28 days. Specimens were tested at 28 days. Alkaline solution: Na <sub>2</sub> SiO <sub>3</sub> + NaOH
0	Uncorroded	0.05-0.11	1.42-1.51	0.04-0.06	
50	Uncorroded	0.25-0.47	1.18-1.68	0.50-0.92	
100	Uncorroded	1.47-2.11	0.30-0.41	0.99-1.46	

d) Alkali activated fly ash materials under ambient environment (Wardhono, Gunasekara, Law, & Setunge, 2017).								
Slag content (%)	Layer	Al/Si						Curing: 80°C at 24 h. Specimens were tested at 28 days and 540 days. Alkaline solution: Na <sub>2</sub> SiO <sub>3</sub> + 15 M NaOH
		28 days	56 days	90 days	180 days	360 days	540 days	
0	Uncorroded	0.23	0.24	0.26	0.27	0.28	0.29	

e) Alkali activated fly ash and OPC under 2% sulfuric acid and ambient environment (Mehta, & Siddique, 2017).					
---	--	--	--	--	--

OPC content (%)	Layer	Na/Al		Al/Si		Ca/Si		Sulfur (%)	
		28	90	28	90	28	90	28	90
0	Corroded	1.76	1.82	0.53	0.48	0.15	0.15	9.52	9.86
	Uncorroded	1.52	1.59	0.44	0.41	0.12	0.10	1.27	1.33
10	Corroded	1.53	1.56	0.85	0.86	0.37	0.49	13.59	16.79
	Uncorroded	1.52	1.49	0.45	0.42	0.23	0.23	1.75	1.02
20	Corroded	1.93	1.82	0.63	0.66	0.76	0.83	18.63	20.35
	Uncorroded	1.36	1.48	0.39	0.38	0.37	0.41	1.64	1.53
30	Corroded	1.83	1.97	0.49	0.45	0.82	0.78	21.47	23.19
	Uncorroded	1.47	1.58	0.31	0.31	0.56	0.63	1.39	1.14

Curing: 80°C at 24 h. Specimens were tested at 28 days. Alkaline solution: Na<sub>2</sub>SiO<sub>3</sub>+10M NaOH (SS/SH:2.5)

f) AAS materials under 5% sodium sulfate and ambient environment (Komljenović, Baščarević, Marjanović, & Nikolić, 2013)

Concrete	Layer	Ca/Si				Al/Si			
		28	28+30	28+60	28+90	28	28+30	28+60	28+90
AAS	Corroded	-	0.7	0.77	0.82	-	0.2	0.26	0.31
	Uncorroded	0.84	0.83	0.8	0.77	0.14	0.19	0.22	0.25

Curing: 20±2 °C; 90±5 RH. Specimens were tested at 28 d. Alkali solution: Na<sub>2</sub>SiO<sub>3</sub>+10M NaOH (SS/SH:2.5)

g) Alkali activated fly ash and slag blends under ambient environment (Marjanović, Komljenović, Baščarević, Nikolić, & Petrović, 2015).

Slag content (%)	Layer	Na/Si	Al/Si	Ca/Si	Curing: 95°C at 24 h. Alkali solution: Na <sub>2</sub> SiO <sub>3</sub> +NaOH
0	Uncorroded	0.31	0.35 (0.19-0.57)	0.12 (0.05-0.24)	
25		0.31	0.4 (0.19-0.57)	0.13 (0.05-0.24)	
50		0.37	0.25 (0.17-0.63)	0.32 (0.21-0.46)	
75		0.29	0.2 (0.15-0.29)	0.4 (0.24-0.52)	
100		0.52	0.13 (0.11-0.16)	0.67 (0.56-0.87)	

#### 4. Conclusions and comments

Geopolymer (100%FA-GPC), alkali-activated fly ash/slag (50%FA+50%S-AFS), and alkali-activated slag (100%S-AAS) concretes can become an environmental solution to ordinary Portland cement (OPC) concrete. For the alkaline solution, sodium silicate and 14 M sodium hydroxide were utilized with a sodium silicate-to-hydroxide ratio of 2.5. The oven-curing was applied for the alkali-activated concretes at 70°C for 48h. The mechanical performance and durability of these concretes were investigated under the 5% sulfuric acid attack, and the microstructural variations were analyzed using SEM/EDS analysis. The following results were obtained in the scope of the research;

1. Visual inspection results indicated that the highest surface deterioration was observed on GPC specimens, while the least surface deterioration was observed on AFS specimens after the 5% sulfuric acid attack. The surface deterioration of the AAS specimen was found less than the degradation of the OPC specimens.
2. Weight loss index (WLI-%) and weight gain index (WGI-%) parameters were proposed and utilized for the weight change results of the specimens after the sulfuric acid attack. The WLI-% and WGI-% yielded weight change results that

became in the range of  $GPC > OPC > AAS > AFS$ . However, the variation in weight becomes smaller in the case of WGI-%, since WGI-% also considers the weight loss due to ongoing geopolymerization reactions in addition to weight loss from acid exposure. Therefore, WGI-% yields more accurate results than WLI-%, especially for ambient cured specimens and GPC specimens.

3. The compressive strength difference between ambient and oven-cured was found negligible for AAS specimens, while the difference was found significant for AFS and GPC specimens. However, the compressive strength values became around 75 MPa, 55 MPa, 50 MPa, and 16 MPa for AAS, AFS, OPC, and GPC specimens, respectively. Results indicated that AAS and AFS specimens can be utilized in structural applications without heat curing even low binder dosages ( $360 \text{ kg/m}^3$ ), while GPC specimens should not be used without heat curing under low fly ash dosages ( $360 \text{ kg/m}^3$ ). Results pointed out that the incorporation of 50% slag was found beneficial to eliminate heat curing.

4. Strength loss index (SLI-%) and strength gain index (SGI-%) parameters were utilized for the compressive strength change after the sulfuric acid attack. The SGI-% results were found different than the SLI-% results due to ongoing geopolymerization reactions. Therefore, SGI-% results were found to be more accurate, which should be used to evaluate the durability of the specimens under chemical exposure. The GPC specimens showed the poorest performance (53% loss), while AFS specimens exhibited superior performance (27% loss) under sulfuric acid attack. Results also indicated that AFS and AAS specimens performed better acid resistance than OPC concrete, while GPC specimens exhibited the poorest acid resistance.

5. SEM/EDS results of the GPC specimens revealed that due to the high amount of unreacted fly ash particles, heterogeneously distributed cavities, and a great number of void and microcracks, GPC specimens showed less dense, porous and permeable microstructure when low fly ash content was utilized ( $360 \text{ kg/m}^3$ ). In addition, the highest reduction in Al/Si atomic ratio was observed in GPC specimens after the acid attack, which can be a result of aluminum leaching due to the proton attack on the Si-O-Al network. Therefore, GPC specimens may exhibit the worst performance against sulfuric acid attacks.

6. SEM/EDS results of the AAS specimens indicated that denser and homogeneous microstructures with reacted slag grains were observed in the AAS specimens. However, wider interconnected macro cracks were observed in the microstructure, which can be attributed to the water evaporation and self-desiccation during heat-curing and shrinkage of the reaction products. In addition to the permeable microstructure, the slight decrease in the Al/Si atomic ratio (loss of aluminum) and high reduction in the Ca/Si atomic ratio (decalcification) can be reasons for the compressive strength loss after the sulfuric acid attack.

7. SEM/EDS results of the AFS specimens showed that the binder phase appears to be denser and homogenous and lacks the self-desiccation cracks as in the AAS specimens. It can be attributed to the extra aluminum from FA particles, which caused stronger and non-granular gel that does not shrink as AAS. AFS microstructure includes fewer cavities and narrower micro cracks with a low amount of unreacted slag and fly ash particles. Therefore, a less porous microstructure is available for AAS and GPC microstructures. In addition, less reduction in Al/Si and Ca/Si atomic ratios were observed after the sulfuric acid attack. Therefore, AFS specimens showed superior performance against sulfuric acid attacks.

**Author contributions:** The contribution of the authors is equal.

**Funding:** The authors received no financial support for this article.

**Acknowledgments:** The authors would like to thank Akcansa Cement Factory, especially Mr. Yasin Engin, for the cement, F-type fly ash, and ground granulated blast furnace slag contributions.

**Conflicts of interest:** On behalf of all authors, the corresponding author states that there is no conflict of interest.

## References

- Albitar, M., Ali, M. M., Visintin, P., & Drechsler, M. (2017). Durability evaluation of geopolymer and conventional concretes. *Construction and Building Materials*, 136, 374-385.
- Allahverdi, A., & Skvara, F. (2001). Nitric acid attack on hardened paste of geopolymeric cements, Part 1. *Ceramics Silikaty*, 45(3), 81-88.
- Allahverdi, A., & Skvara, F. (2005). Sulfuric acid attack on hardened paste of geopolymer cements-Part 1. Mechanism of corrosion at relatively high concentrations. *Ceramics Silikaty*, 49(4), 225.

- Al-Majidi, M. H., Lampropoulos, A., Cundy, A., & Meikle, S. (2016). Development of geopolymer mortar under ambient temperature for in situ applications. *Construction and Building Materials*, 120, 198-211.
- ASTM C39/C39M-01. (2003). Standard test method for compressive strength of cylindrical concrete specimens. *Am. Soc. Test. Mater. West Conshohocken, USA*.
- ASTM, C618-03. (2003). Standard specification for coal fly ash and raw or calcined natural pozzolan for use in concrete.
- Attiogbe, E. K., & Rizkalla, S. H. (1988). Response of concrete to sulfuric acid attack. *ACI materials journal*, 85(6), 481-488.
- Aygormez, Y. (2021). Sulfuric acid effect and application of freezing-thawing curing on long fiber reinforced metabentonite and slag-based geopolymer composites. *Advances in concrete construction*, 12(2), 145-156.
- Aygormez, Y., & Canpolat, O. (2021). Long-term sulfuric and hydrochloric acid resistance of silica fume and colemanite waste reinforced metakaolin-based geopolymers. *Revista de la construcción*, 20(2), 291-307.
- Bakharev, T. (2005). Geopolymeric materials prepared using Class F fly ash and elevated temperature curing. *Cement and concrete research*, 35(6), 1224-1232.
- Bassuoni, M. T., & Nehdi, M. L. (2007). Resistance of self-consolidating concrete to sulfuric acid attack with consecutive pH reduction. *Cement and Concrete Research*, 37(7), 1070-1084.
- Benhelal, E., Zahedi, G., Shamsaei, E., & Bahadori, A. (2013). Global strategies and potentials to curb CO<sub>2</sub> emissions in cement industry. *Journal of cleaner production*, 51, 142-161.
- Bondar, D., Lynsdale, C. J., Milestone, N. B., Hassani, N., & Ramezaniyanpour, A. A. (2011). Effect of type, form, and dosage of activators on strength of alkali-activated natural pozzolans. *Cement and Concrete Composites*, 33(2), 251-260.
- Chang, Z. T., Song, X. J., Munn, R., & Marosszeky, M. (2005). Using limestone aggregates and different cements for enhancing resistance of concrete to sulphuric acid attack. *Cement and Concrete Research*, 35(8), 1486-1494.
- Chi, M., & Huang, R. (2013). Binding mechanism and properties of alkali-activated fly ash/slag mortars. *Construction and Building Materials*, 40, 291-298.
- Çevik, A., Alzeebaree, R., Humur, G., Niş, A., & Gülşan, M. E. (2018). Effect of nano-silica on the chemical durability and mechanical performance of fly ash based geopolymer concrete. *Ceramics International*, 44(11), 12253-12264.
- Džunuzović, N., Komljenović, M., Nikolić, V., & Ivanović, T. (2017). External sulfate attack on alkali-activated fly ash-blast furnace slag composite. *Construction and Building Materials*, 157, 737-747.
- European Committee for Standardization. EN 206-1:2013, Concrete—Specification, Performance, Production and Conformity; CEN: Brussels, Belgium, 2013.
- Fernández-Jiménez, A., Palomo, A., & Criado, M. (2005). Microstructure development of alkali-activated fly ash cement: a descriptive model. *Cement and concrete research*, 35(6), 1204-1209.
- Gao, K., Lin, K. L., Wang, D., Hwang, C. L., Shiu, H. S., Chang, Y. M., & Cheng, T. W. (2014). Effects SiO<sub>2</sub>/Na<sub>2</sub>O molar ratio on mechanical properties and the microstructure of nano-SiO<sub>2</sub> metakaolin-based geopolymers. *Construction and Building Materials*, 53, 503-510.
- Golewski, G. L., & Sadowski, T. (2017). The fracture toughness the KIIC of concretes with F fly ash (FA) additive. *Construction and Building Materials*, 143, 444-454.
- Imbabi, M. S., Carrigan, C., & McKenna, S. (2012). Trends and developments in green cement and concrete technology. *International Journal of Sustainable Built Environment*, 1(2), 194-216.
- Ibrahim, M., Johari, M. A. M., Rahman, M. K., & Maslehuddin, M. (2017). Effect of alkaline activators and binder content on the properties of natural pozzolan-based alkali activated concrete. *Construction and Building Materials*, 147, 648-660.
- Ismail, I., Bernal, S. A., Provis, J. L., San Nicolas, R., Hamdan, S., & van Deventer, J. S. (2014). Modification of phase evolution in alkali-activated blast furnace slag by the incorporation of fly ash. *Cement and Concrete Composites*, 45, 125-135.
- Jang, J. G., Lee, N. K., & Lee, H. K. (2014). Fresh and hardened properties of alkali-activated fly ash/slag pastes with superplasticizers. *Construction and Building Materials*, 50, 169-176.
- Juenger, M. C. G., Winnefeld, F., Provis, J. L., & Ideker, J. H. (2011). Advances in alternative cementitious binders. *Cement and concrete Research*, 41(12), 1232-1243.
- Komljenović, M., Baščarević, Z., Marjanović, N., & Nikolić, V. (2013). External sulfate attack on alkali-activated slag. *Construction and Building Materials*, 49, 31-39.
- Kumar, R., Kumar, S., & Mehrotra, S. P. (2007). Towards sustainable solutions for fly ash through mechanical activation. *Resources, Conservation and Recycling*, 52(2), 157-179.

- Kumaravel, S., & Girija, K. (2013). Acid and salt resistance of geopolymer concrete with varying concentration of NaOH. *Journal of Engineering Research and Studies*, 4(4), 1-3.
- Kurtoglu, A. E., Alzebaree, R., Aljumaili, O., Nis, A., Gulsan, M. E., Humur, G., & Cevik, A. (2018). Mechanical and durability properties of fly ash and slag based geopolymer concrete. *Advances in Concrete Construction*, 6(4), 345-362.
- Lee, N. K., Jang, J. G., & Lee, H. K. (2014). Shrinkage characteristics of alkali-activated fly ash/slag paste and mortar at early ages. *Cement and Concrete Composites*, 53, 239-248.
- Li, S., & Roy, D. M. (1988). Preparation and characterization of high and low CaO/SiO<sub>2</sub> ratio "pure" C-S-H for chemically bonded ceramics. *Journal of Materials Research*, 3(2), 380-386.
- Li, Z., & Ding, Z. (2003). Property improvement of Portland cement by incorporating with metakaolin and slag. *Cement and Concrete Research*, 33(4), 579-584.
- Ma, C. K., Awang, A. Z., & Omar, W. (2018). Structural and material performance of geopolymer concrete: A review. *Construction and Building Materials*, 186, 90-102.
- Marjanović, N., Komljenović, M., Baščarević, Z., Nikolić, V., & Petrović, R. (2015). Physical-mechanical and microstructural properties of alkali-activated fly ash-blast furnace slag blends. *Ceramics International*, 41(1), 1421-1435.
- Mehta, A., & Siddique, R. (2017). Sulfuric acid resistance of fly ash based geopolymer concrete. *Construction and Building Materials*, 146, 136-143.
- Niš, A., & Altundal, İ. (2021). Compressive Strength Performance of Alkali Activated Concretes under Different Curing Conditions. *Periodica Polytechnica Civil Engineering*, 65(2), 556-565.
- Palomo, A., Grutzeck, M. W., & Blanco, M. T. (1999). Alkali-activated fly ashes: a cement for the future. *Cement and concrete research*, 29(8), 1323-1329.
- Part, W. K., Ramli, M., & Cheah, C. B. (2015). An overview on the influence of various factors on the properties of geopolymer concrete derived from industrial by-products. *Construction and Building Materials*, 77, 370-395.
- Patil, A. A., Chore, H. S., & Dodeb, P. A. (2014). Effect of curing condition on strength of geopolymer concrete. *Advances in concrete construction*, 2(1), 29-37.
- Provis, J. L., Myers, R. J., White, C. E., Rose, V., & van Deventer, J. S. (2012). X-ray microtomography shows pore structure and tortuosity in alkali-activated binders. *Cement and Concrete Research*, 42(6), 855-864.
- Puertas, F., Martínez-Ramírez, S., Alonso, S., & Vazquez, T. (2000). Alkali-activated fly ash/slag cements: strength behaviour and hydration products. *Cement and Concrete Research*, 30(10), 1625-1632.
- Reddy, M. S., Dinakar, P., & Rao, B. H. (2018). Mix design development of fly ash and ground granulated blast furnace slag based geopolymer concrete. *Journal of Building Engineering*, 20, 712-722.
- Riditirud, C., Chindaprasirt, P., & Pimraksa, K. (2011). Factors affecting the shrinkage of fly ash geopolymers. *International Journal of Minerals, Metallurgy, and Materials*, 18(1), 100-104.
- Ryu, G. S., Lee, Y. B., Koh, K. T., & Chung, Y. S. (2013). The mechanical properties of fly ash-based geopolymer concrete with alkaline activators. *Construction and Building Materials*, 47, 409-418.
- Soutsos, M., Boyle, A. P., Vinai, R., Hadjierakleous, A., & Barnett, S. J. (2016). Factors influencing the compressive strength of fly ash based geopolymers. *Construction and Building Materials*, 110, 355-368.
- Tavasoli, S., Nili, M., & Serpoosh, B. (2018). Effect of GGBS on the frost resistance of self-consolidating concrete. *Construction and Building Materials*, 165, 717-722.
- Temujin, J. V., Van Riessen, A., & Williams, R. (2009). Influence of calcium compounds on the mechanical properties of fly ash geopolymer pastes. *Journal of hazardous materials*, 167(1-3), 82-88.
- Thokchom, S. (2014). Fly ash geopolymer pastes in sulphuric acid. *Int. J. Eng. Innovation Res*, 3(6), 943-947.
- TS13515 (2012). Complementary standard for application of TS EN 206-1.
- Wardhono, A., Gunasekara, C., Law, D. W., & Setunge, S. (2017). Comparison of long term performance between alkali activated slag and fly ash geopolymer concretes. *Construction and Building materials*, 143, 272-279.
- Winnefeld, F., Leemann, A., Lucuk, M., Svoboda, P., & Neuroth, M. (2010). Assessment of phase formation in alkali activated low and high calcium fly ashes in building materials. *Construction and building materials*, 24(6), 1086-1093.
- Wongpa, J., Kiattikomol, K., Jaturapitakkul, C., & Chindaprasirt, P. (2010). Compressive strength, modulus of elasticity, and water permeability of inorganic polymer concrete. *Materials & Design*, 31(10), 4748-4754.
- Zhang, W., Yao, X., Yang, T., & Zhang, Z. (2018). The degradation mechanisms of alkali-activated fly ash/slag blend cements exposed to sulphuric acid. *Construction and Building Materials*, 186, 1177-1187.



Copyright (c) 2023 Author., Co-Author, Co-Author. This work is licensed under a [Creative Commons Attribution-Noncommercial-No Derivatives 4.0 International License](https://creativecommons.org/licenses/by-nc-nd/4.0/).